






Article

Treatment of Effluent Containing p-Cresol through an Advanced Oxidation Process in a Batch Reactor: Kinetic Optimization

Julierme G. C. Oliveira ¹, Yana B. Brandão ^{2,3,4}, Dinaldo C. Oliveira ³, Jailson R. Teodosio ¹, Cristiane M. Moraes ³, Attilio Converti ⁵, Alessandro Alberto Casazza ^{5,*}, Leonie Asfora Sarubbo ^{1,3,4} and Mohand Benachour ^{3,4}

¹ Department of Chemical Engineering, Catholic University of Pernambuco (UNICAP), Rua do Príncipe, 526, Recife 50050-900, Brazil; julierme.oliveira@unicap.br (J.G.C.O.); jailson.rolim@unicap.br (J.R.T.); leonie.sarubbo@unicap.br (L.A.S.)

² Department of Engineering, Federal Rural University of Pernambuco (UFRPE), UACSA, Cabo de Santo Agostinho 54518-430, Brazil; yana.brandao@ufrpe.br

³ Department of Chemical Engineering and Clinical Medicine, Federal University of Pernambuco (UFPE), Av. dos Economistas, s/n, Recife 50740-590, Brazil; dinaldo@cardiol.br (D.C.O.); cristiane3301@hotmail.com (C.M.M.); mbena@ufpe.br (M.B.)

⁴ Instituto Avançado de Tecnologia e Inovação (IATI), Rua Potyra, 31, Recife 50751-310, Brazil

⁵ Department of Civil, Chemical and Environmental Engineering, University of Genoa (UNIGE), I-16145 Genoa, Italy; converti@unige.it

* Correspondence: alessandro.casazza@unige.it

Abstract: The present research is related to the study of p-cresol oxidation reaction in aqueous phase. Firstly, the conventional advanced oxidation process (AOP) in a lab-scale batch reactor was used, seeking to identify the most impacting process variables and then to propose an optimization approach for ensuring the complete p-cresol degradation and the highest total organic carbon (TOC) conversion. In the AOP with the use of hydrogen peroxide as the oxidizing agent, the oxidation reaction was optimized with the aid of a factorial design, and a maximum TOC conversion of 63% was obtained. The Lumped Kinetic Model (LKM) was used to describe the profile of residual TOC concentration due to chemical species, which were categorized into two groups (refractory and non-refractory compounds). The model was able to satisfactorily describe the profile of the residual fractions of these two classes of organic compounds and allowed estimating the related kinetic constants (k) at two different temperatures, namely (a) 3.19×10^{-1} and $2.82 \times 10^{-3} \text{ min}^{-1}$ for non-refractory and refractory compounds at 80 °C and (b) 4.73×10^{-1} and $5.09 \times 10^{-3} \text{ min}^{-1}$ for the same compound classes at 90 °C, while the activation energy (E_a) of the process was 42.02 and 62.09 kJ mol⁻¹, respectively. The kinetic modeling of organic pollutants oxidation in liquid effluents would allow to perform in situ seawater treatment on vertical reactors installed in offshore platforms and to properly release treated water into the oceans. In this way, ocean contamination caused by the exploration on offshore platforms of oil and natural gas, the main energy sources and vectors in the current world, may be remarkably reduced, thus favoring a more eco-friendly energy production.

Keywords: p-cresol; HPLC; total organic carbon; advanced oxidation process; Lumped Kinetic Model



Citation: Oliveira, J.G.C.; Brandão, Y.B.; Oliveira, D.C.; Teodosio, J.R.; Moraes, C.M.; Converti, A.; Casazza, A.A.; Sarubbo, L.A.; Benachour, M. Treatment of Effluent Containing p-Cresol through an Advanced Oxidation Process in a Batch Reactor: Kinetic Optimization. *Energies* **2023**, *16*, 5027. <https://doi.org/10.3390/en16135027>

Academic Editor: Ronghou Liu

Received: 1 June 2023

Revised: 14 June 2023

Accepted: 25 June 2023

Published: 28 June 2023



Copyright: © 2023 by the authors. Licensee MDPI, Basel, Switzerland. This article is an open access article distributed under the terms and conditions of the Creative Commons Attribution (CC BY) license (<https://creativecommons.org/licenses/by/4.0/>).

1. Introduction

Energy production in offshore platforms, which are commonly used to drill oil and natural gas, becomes increasingly significant from the environmental point of view due to large emissions of carbon dioxide (CO₂) and nitrogen oxides (NO_x), which are responsible for the greenhouse effect [1]. Currently, analyses and studies on offshore platforms, such as those located in the North Sea, are being intensified [2].

Natural gas (NG), an energy source mainly composed of methane, has been widely consumed around the world. Even though its combustion leads to CO₂ emission as

well, it has been conceptualized as a fundamental energy source for the future and is largely available in petroleum fields throughout the planet. Therefore, NG is used in several applications, which increases its consumption every day [3]. This implies that the generation of energy becomes a concern for the planet, due once again to the impacts caused for the environment, especially in terms of disposal of residues remaining after the extraction of both oil and natural gas from petroleum fields.

Water injected for oil and natural gas recovery in most offshore platforms is contaminated, after use, by 80% of organic and inorganic refractory substances [4], which are either dispersed or dissolved [5]. The dispersed components most often consist of small suspended oil droplets, which are treated conventionally, while the dissolved ones are polar components with a medium or low number of carbons [6–8]. However, many of these refractory and organic effluents cannot be treated conventionally [9].

Petroleum is a complex mixture of numerous compounds, most of them being hydrocarbons. Their proportion varies from one oil field to another depending on the nature of the oil [10]. Typically, chemical and aromatic compounds can be found in wastewater from chemical and petrochemical industries, such as coal, phenolic effluents, pharmaceutical, metal coating, polymers, resins, textiles, pulp and paper, oil refinery, and agricultural activities [11]. Therefore, to destroy these chemical compounds and reduce environment pollution, several technologies have been implemented, such as adsorption, ozonization, extraction, chemical oxidation, electrochemical treatments, and advanced oxidation processes, among others. However, sometimes these processes need to be improved due to some requirements, as they can have high cost and low efficiency, or can lead to the formation of dangerous and toxic byproducts [12].

The treatment of aqueous streams containing toxic organic and refractory substances has been a great challenge mainly due to the presence of phenolic compounds, whose concentration depends on the type of effluents, such as sidestreams of oil refinery (100–250 mg L⁻¹), untreated wastewater from oil refinery (10–50 mg L⁻¹), coke plants (250–3000 mg L⁻¹), the wood preserving industry (25–350 mg L⁻¹), and aircraft paint stripping (1000–3000 mg L⁻¹) [13].

Phenols and p-cresols are considered priority pollutants by the US Environmental Protection Agency (EPA) due to their toxicity to humans and animals; severe exposure to them can in fact lead to damage to the functions of the blood, liver, kidney, nervous system, and heart, and can affect the eyes, lungs, skin, stomach, and brain [14,15]. Phenols are usually found in a colorless solid state under normal conditions of temperature and pressure, but they have a very typical intense smell when present in their simplest monomeric form. Cresols, the methylated derivatives of phenol, are composed of different isomers according to the position of the methyl group, including the leading para (p-) one [16].

Some accidental leaks, such as those that occurred in the Port of Gothenburg (Sweden) and the Xin'an River (China), provoked the release of huge amounts of phenols and cresols into the aquatic ecosystem, posing a threat to the water quality in these regions and nearby places [17,18]. Due to the high solubility of phenols and cresols in water (8.28 g/100 mL and 2.15–2.60 g/100 mL, respectively), they can persist in high concentrations in the aquatic ecosystem [19]. Moreover, phenols, when present in drinking water in a concentration of 1 mg L⁻¹, can also cause significant harm to humans, as well as the death of fish even at lower concentrations [20]. Recently, the aquatic environment has been largely monitored by remote sensing and geostatistics to solve the problems arisen in several cities due to the pollution of their water resources generated by huge urbanization. These studies have great importance to improve aquatic ecosystem management [21]. Another source of environmental pollution refers to the presence of high levels of microplastics in the aquatic environment, as it has been found, for example, in the Maowei Sea and surrounding waters. In this area, a study was carried out to evaluate the environmental impact of pollutants from aquaculture on the sea using data from satellite remote detecting, unoccupied aerial vehicles, in situ tests, and classification by questionnaires. This study

showed the importance for the aquaculture sector of intensifying the monitoring and management of microplastics [22].

Volatile organic compounds (VOCs), coming from natural and anthropogenic sources, are also classified as another category of hazardous pollutants. P-Cresol, belonging also to this class, is present in domestic, agricultural, and industrial wastewater and is considered a toxic and carcinogenic phenolic by the EPA [23,24]. Therefore, analyzing water bodies becomes increasingly important due to the possibility of finding these emerging contaminants that are harmful to human health and the environment [25,26].

Cresols and phenolic derivatives have had an intense impact on the aquatic ecosystem due to the release of heavily polluted wastewater. For this reason, several physicochemical and biodegradation processes have been used to treat industrial effluents containing these organic refractory compounds, such as ozonization, adsorption, photocatalysis, use of membranes, and enzymatic treatment [27].

Advanced oxidation processes (AOPs) are a technology that, in recent years, has been widely used to treat effluents containing refractory organic substances, in addition to the other existing consolidated biological, physical, and chemical processes. Among the techniques that use AOPs, the use of ozone combined with hydrogen peroxide (O_3/H_2O_2) and/or with ultraviolet radiation (O_3/UV and $O_3/UV/H_2O_2$) has been highlighted. Another possibility of using AOPs in the treatment of organic effluents is through the physicochemical, Fenton and Fenton-like techniques. The main determination in the application of these AOP-based techniques is the possibility of destroying a refractory compound or even converting it or its derivatives into biodegradable compounds thanks to the formation of hydroxyl radical ($\bullet OH$), which is an effective species in decomposing a large part of organic pollutants [28].

AOPs have been used in combination with oxidants in techniques that give rise to several intermediate steps with the formation of $\bullet OH$, this species being unstable and likely to react easily due to its oxidizing power (2.8 V) in an acidic medium. These processes mineralize into carbon dioxide and water practically all intermediates from the reaction of refractory compounds, which cannot be decomposed through other conventional methods [29].

Perovskite-based oxides, when used in AOPs, showed high catalytic efficiency thanks to the possible formation of both free and non-free radicals in the reaction medium. These oxides have been investigated in Ruddlesden–Popper layers to stimulate peroxymonosulfate (PMS) in generating reactive oxygen species with high activity and mobility, enabling the formation of non-free radical singlet oxygen in AOPs that leads to $LaSrCo_{0.8}Fe_{0.2}O_4$, which is highly effective in PMS [30]. Non-free Fe was used in the electro-Fenton process applying rod-shaped erdite for PMS stimulation in an electric field for enhancing the process efficiency in neutral wastewater. During erdite hydrolysis, free radicals ($\bullet OH$ and $\bullet SO_4^-$) formed increasing p-nitrophenol removal efficiency using erdite/PMS and erdite/PMS/electric field [31].

Hydrogen peroxide is also widely used in AOPs as a strong oxidizing agent during the degradation of certain refractory chemicals. However, data reported in the literature show that its greatest efficiency occurs when it is used in a combined way, such as a H_2O_2/UV or $H_2O_2/catalyst$ [32,33]. These methods have been effective in oxidative systems, according to the wastewater to be treated, because of the chemical reactions that take place during the decomposition of organic pollutants [34,35]. AOPs have also been used after pre-magnetization to treat refractory effluents, due to the effectiveness of radicals ($\bullet OH$ and $\bullet SO_4^-$) in degrading recalcitrant organic compounds into others with lower toxicity potential [36].

The legislation of the Conselho Nacional do Meio Ambiente—CONAMA (National Council on the Environment, resolution No. 430, published on 13 May 2011, Brazil) established a maximum threshold concentration of total phenols of 0.5 mg L^{-1} in all effluents originating from any polluting source that can be released into water bodies [37].

The evaluation of the oxidation kinetics of these organic compounds becomes fundamental to develop processes for the in situ treatment of these pollutants in seawaters, using vertical reactors on offshore platforms in the prospection and production of oil and natural gas. Such energy sources are, in fact, still essential for any current human activity on the planet, waiting for a significant growth of the generation of alternative energies, such as wind, solar, biomass, and nuclear energies, among others. The quantification of kinetic constants is of paramount importance in the design of gas/liquid reactors, which are made up of vertical reaction absorption columns to be used in situ that occupy little space on offshore platforms. Therefore, natural gas could be used as an energy source for the treatment process, thus respecting the concept of cleaner and more sustainable technologies.

The aim of this study was to identify the most significant process variables and propose an optimization approach for complete p-cresol degradation and maximum TOC conversion. It was focused on the investigation in a lab-scale batch reactor of p-cresol oxidation in aqueous phase at 1.0 bar pressure using an AOP. For this purpose, the research was divided into two stages, in the first of which a factorial design was employed to identify the optimal conditions of batch p-cresol oxidation, while in the second one, the kinetic parameters of this reaction were determined. No work has yet investigated, as far as we are aware, the performance of using H_2O_2 as a source of free $\bullet\text{OH}$ for p-cresol degradation and TOC reduction through an AOP in a batch reactor with kinetic optimization. The kinetic model used to describe the profile of the TOC conversion was the Lumped Kinetic Model (LKM).

2. Materials and Methods

2.1. Chemicals

Laboratory tests were performed in a batch reactor using a model solution containing p-cresol (99% analytical grade (AR), ASC Científica, Belém, PA, Brazil), while the oxidizing agent was a water solution of hydrogen peroxide (35% AR, Vetec, Duque de Caxias, RJ, Brazil). Methanol (UV/HPLC, 99.9% AR, Vetec) was used in high-performance liquid chromatography (HPLC) to determine the concentrations of analytes, while a 25% phosphoric acid solution (AR, Vetec) was used for the TOC analysis [20].

2.2. Experimental Setup

Figure 1 shows a photograph of the 1.8-L stainless steel batch reactor (model 4848, Parr Co., Moline, IL, USA) used in the experiments. It is provided with an electronic system for monitoring and controlling the mechanical agitation speed, pressure, and temperature at the selected constant values (see later), and was used with a working volume of 1.3 L. Temperature was regulated through a heating blanket available as an accessory in the reactor.

Initially, a synthetic liquid effluent with an initial p-cresol concentration of 500 mg L^{-1} was prepared by dissolving 0.6489 g of p-cresol in 1.3 L of distilled water and transferred to the cylindrical body of the batch reactor. The rotational speed and pressure were set, according to Teodosio [29], at 500 rpm and 1.0 kgf cm^{-2} (1.0 bar), respectively, while temperature (T), air flowrate (F), and molar p-cresol/ H_2O_2 stoichiometric ratio (R) were set at values selected for the factorial design, namely 60 to 90 °C, 50 to 150 L h^{-1} , and 25 to 98%. H_2O_2 was added as the oxidizing agent inside the reactor to start the oxidation of p-cresol solution. In each experiment, 30 mL of the solution was collected in triplicate at time intervals of 45 min up to 3 h. All the samples were collected in amber glass bottles and then refrigerated. A sample of 30 mL of treated water without p-cresol was used as the analytical blank.



Figure 1. Photograph of the batch reactor used for p-cresol oxidation experiments.

2.3. Analytical Methods

2.3.1. High-Performance Liquid Chromatography (HPLC)

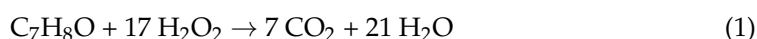
The HPLC equipment used was a Shimadzu Prominence (prototypical LC-20AT) provided with pump, DGU-20As degasser, CBM-20A module, SPD-20A/UV/VIS detector and CTO-20A oven (Shimadzu, Kyoto, Japan). A CLC-ODS(M)/(C-18) column (Shimadzu) with 250 mm in length and 4.6 mm in diameter was used in isocratic mode to detect p-cresol. For this purpose, the furnace temperature was maintained at 40 °C, the injection volume was 20 µL, the mobile phase had a constant composition of 40% methanol and 60% water (Milli-Q), the flow rate of the mobile phase was 1.0 mL min⁻¹, and the wavelength of the UV detector was set at 254 nm [20,29].

2.3.2. Total Organic Carbon (TOC)

TOC conversion was analyzed with a TOC-VCSH prototypical analyzer (Shimadzu) with high sensitivity catalyst (4 ppb–25,000 ppm) to quantify p-cresol mineralization. This equipment is able to simultaneously quantify TOC, total inorganic carbon (TIC), total carbon (TC), and total nitrogen (TN), and the TOC level is given by subtracting the TIC level from that of TC. During the determination of TIC, the sample reacts with 25% phosphoric acid, and all inorganic carbon is converted to CO₂, which is quantified by absorption in the non-dispersive infrared detector [28,29].

2.4. Definition of Response Variables

The 100% stoichiometric molar ratio of p-cresol to oxidizing agent H₂O₂ represents the complete mineralization (transformation into CO₂ and H₂O) of p-cresol (brute formula C₇H₈O), according to the reaction described by the Equation (1):



Molar ratios other than 100% were established proportionally, as predicted by the above stoichiometry.

The degradation of p-cresol, C_{A0} (%), ensured by the AOP, expressed as a percentage (%), was calculated according to Equation (2):

$$C_{A0}(\%) = \frac{C_0 - C}{C_0} \times 100 \quad (2)$$

where C_0 and C are p-cresol concentrations in the liquid effluent at the beginning and at a given time, respectively. This response achieved its maximum value after the time ensuring the lowest values of C .

The TOC conversion, TOC (%), expressed as a percentage (%), was described by Equation (3):

$$TOC(\%) = \frac{TOC_0 - TOC}{TOC_0 - TOC_B} \times 100 \quad (3)$$

where TOC_0 and TOC are the total organic carbon in the liquid effluent at the beginning and at a given time, respectively, while TOC_B that in pure water (blank). The maximum value of this response was obtained when the organic compound was completely mineralized to CO_2 and H_2O .

2.5. Statistical Techniques and Optimization of Kinetic Variables

In the first phase, experiments were performed according to a 2^3 -full factorial design with 3 factors (k) and 2 levels and the addition of four repetitions at the central point, totaling 12 runs, and samples were collected after times (t) of 45, 90, 135, and 180 min. The Statistica 8.0 software package for Windows (StatSoft, Tulsa, OK, USA) was used for statistical analysis. Since the most prevalent models for graph generation using Response Surface Methodology (RSM) are second-order ones, they were used to fit and illustrate the experimental data [20,34]. A 2^3 -full factorial design was preferred because, according to literature, it should be effective in optimization being able to adjust a quadratic model for RSM [38]. Three independent variables were initially selected, namely T , F , and R , whose actual values were 60, 70, and 80 °C; 50, 100, and 150 $L\ h^{-1}$; and 25, 50, and 75%, respectively, corresponding to coded levels of -1 , 0 , and $+1$. Table 1 shows the matrix of the 2^3 -full factorial design.

Table 1. Matrix of the 2^3 -full factorial design with four central points used to optimize p-cresol degradation, with coded levels written between brackets. The reaction time was 180 min.

Run	T (°C)	R (%)	F ($L\ h^{-1}$)
1	60 (−1)	25 (−1)	50 (−1)
2	80 (+1)	25 (−1)	50 (−1)
3	60 (−1)	75 (+1)	50 (−1)
4	80 (+1)	75 (+1)	50 (−1)
5	60 (−1)	25 (−1)	150 (+1)
6	80 (+1)	25 (−1)	150 (+1)
7	60 (−1)	75 (+1)	150 (+1)
8	80 (+1)	75 (+1)	150 (+1)
9 *	70 (0)	50 (0)	100 (0)
10 *	70 (0)	50 (0)	100 (0)
11 *	70 (0)	50 (0)	100 (0)
12 *	70 (0)	50 (0)	100 (0)

* Central point runs; T = reaction temperature; R = molar stoichiometric ratio of p-cresol/hydrogen peroxide; F = air flowrate.

A similar 2^3 -factorial design was successfully applied by Brandão et al. [20] to the thermochemical AOP called direct contact thermal treatment (DiCTT) for phenol degradation and TOC conversion. For this purpose, the authors used initial phenol concentration (500, 1000, and 1500 $mg\ L^{-1}$), molar stoichiometric ratio of phenol/hydrogen peroxide (25, 50,

and 75%), and treatment time (30, 90, and 150 min) as the independent variables, and the response surface methodology (RSM) as a design tool to optimize the process and analyze the system performance [39].

In the second phase, the Maximum Ascending Gradient Method (MAGM) was used with the same variables (T, R, and F) to obtain the point considered optimal for TOC conversion. Table 2 shows the matrix of the experimental design used to map the region where it exhibited an inflection point.

Table 2. Matrix of the MAGM experimental design used to select the conditions for optimal TOC conversion. The reaction time was 180 min.

Run	T (°C)	R (%)	F (L h ⁻¹)
1	70	50	100
2	80	57	105
3	90	64	110
4	90	71	115
5	90	78	120
6	90	85	125
7	90	92	130
8	90	100	135

T = reaction temperature; R = molar stoichiometric ratio of p-cresol/hydrogen peroxide; F = air flowrate.

Teodosio et al. [29] were successful in applying the same MAGM technique to treat a hydroquinone solution by a homogeneous AOP of the peroxidation type, in a batch reactor, using the initial pH (4, 7, and 10), temperature of the effluent (60, 70, and 80 °C), air flowrate (50, 100, and 150 L h⁻¹) and molar stoichiometric ratio of hydroquinone/hydrogen peroxide (25, 50, and 75%) as the independent variables. Optimal conditions for maximal TOC conversion were easily revealed by the occurrence of a maximum point.

In the third phase, using the point of maximum upward inclination selected by the MAGM technique, at temperature of 90 °C and reaction time of 180 min, we applied a new 2²-full factorial design with the addition of four repetitions at the central point, totaling 8 runs. For this purpose, R and F were selected as the independent variables at levels determined in the trial project (64, 78, and 92% for the former, and 110, 120, and 130 L h⁻¹ for the latter), both corresponding to coded levels of -1, 0, and +1. Table 3 shows the matrix of this 2²-full factorial design.

Table 3. Matrix of the 2²-full factorial design with four central points used to optimize TOC conversion, with coded levels written between brackets. The reaction time and temperature were 180 min and 90 °C, respectively.

Run	R (%)	F (L h ⁻¹)
1	64 (-1)	110 (-1)
2	64 (-1)	130 (+1)
3	92 (+1)	110 (-1)
4	92 (+1)	130 (+1)
5 *	78 (0)	120 (0)
6 *	78 (0)	120 (0)
7 *	78 (0)	120 (0)
8 *	78 (0)	120 (0)

* Central point runs; R = molar stoichiometric ratio of p-cresol/hydrogen peroxide; F = air flowrate.

In this fourth final phase, the results obtained from this procedure were submitted to statistical analysis using the Statistic 8.0 software package for Windows (Statsoft). Since it revealed lack of adjustment to the linear model, a Rotational Central Composite Design (RCCD) was then performed at the same temperature and reaction time to know whether the latter ranges of independent variables contained the maximum conversion point. For

this, 5 runs were performed aiming to complement the 8 runs of the 2^2 -full factorial design (Table 3). For this purpose, although the selected independent variables were the same, their ranges were enlarged with the axial points ($R = 58$ and 98% , $F = 106$ and 134 L h^{-1} , corresponding to coded levels of -1.41 and $+1.41$), while keeping the same central point conditions ($R = 78\%$, $F = 120 \text{ L h}^{-1}$). Table 4 shows the matrix of complementing runs carried out according to this RCCD.

Table 4. Matrix of runs carried out according to the RCCD, with coded levels written between bracket. The reaction time and temperature were 180 min and 90°C , respectively.

Run	R (%)	F (L h ⁻¹)
1	58 (−1.41)	120 (0)
2	78 (0)	106 (−1.41)
3	98 (+1.41)	120 (0)
4	78 (0)	134 (+1.41)
5	78 (0)	120 (0)

R = molar stoichiometric ratio of p-cresol/hydrogen peroxide; F = air flowrate.

In the fifth phase, the Desirability Function Method was used with the same variables (R and F) to obtain optimization for TOC conversion that were submitted to statistical analysis using the Statistic 8.0 software package.

The Desirability function is a tool used to optimize an interest variable. Proposed by Harrington [40], it allows to describe the output variable as a function of input variables and presents response from normalized values ($0 \leq d \leq 1$). Desirability is favored as the response moves away from zero, reaching maximum desirability value with unit value.

Derringer and Suich [41] modified the original Desirability function and defined optimization functions of three classes: *STB* (smaller-the-better), *LTB* (larger-the-better), and *NTB* (nominal-the-better). They assumed a response variable (y) with lower specification limit (*LSL*) and upper specification limit (*USL*). The *STB* function seeks to minimize y , while the *LTB* function seeks to maximize y . The *NTB* function seeks to optimize from a target value (λ). The different Desirability functions are defined as:

$$d_{STB} = \begin{cases} \left| \frac{y-LSL}{\alpha-LSL} \right|^\tau & (\alpha \leq y \leq USL) \\ 0 & (y > USL) \end{cases} \quad (4)$$

$$d_{LTB} = \begin{cases} 0 & (y < LSL) \\ \left| \frac{y-LSL}{USL-LSL} \right|^\tau & (LSL \leq y \leq USL) \\ 1 & (y > USL) \end{cases} \quad (5)$$

$$d_{NTB} = \begin{cases} 0 & (y < LSL \text{ ou } y > USL) \\ \left| \frac{y-LSL}{\lambda-LSL} \right|^s & (LSL \leq y \leq \lambda) \\ \left| \frac{y-USL}{\lambda-USL} \right|^\tau & (\lambda \leq y \leq USL) \end{cases} \quad (6)$$

where α is the smallest possible value for the response variable (y) and λ is the nominal (target) value for y . The parameters τ and s are constants of the Desirability function (0.01 to 10).

The first step in applying the Desirability function is to establish an optimal regression equation for predicting the response variable. The parameters of the regression can be obtained by the method of least squares (MLS) and the verification of its (optimized) condition is performed with ANOVA and the F-test (significance) [42,43]. The three methods are available in Statistic 8.0 software.

2.6. Kinetic Modeling of p-Cresol Degradation

In the scientific literature, it is possible to find many kinetic models applied to reactions involving multicomponent systems, mainly using Chemical Oxygen Demand (COD), Biochemical Oxygen Demand (BOD), or Total Organic Carbon (TOC) to express the concentration of organic pollutants [44,45]. This choice is due to the great difficulty of tracking and quantifying the degradation of each chemical species involved in the complex reaction mechanisms characteristic of AOPs [29].

A model of special interest to describe TOC conversion along the time is the Lumped Kinetic Model (LKM) proposed by Li et al. [29,46]. This model, originally developed to investigate the catalytic wet oxidation of organic compounds, has been successful in describing the profile of total residual concentration in terms of carbon contained in the liquid phase.

Thus, in the sixth phase of this work, the LKM was applied to TOC conversion to get the kinetic model for p-cresol oxidation. For this purpose, the oxidation of organic components is assumed to occur in parallel steps, according to the scheme of Equations (7) and (8):



where A is the contaminant (p-cresol) plus non-refractory intermediates, B are refractory organic intermediates compounds resulting from A oxidation, and C is carbon dioxide generated from total mineralization.

The mass balances for all groups of species are defined by Equations (9)–(11):

$$\frac{dC_A}{dt} = -(k_1 + k_3)C_A \tag{9}$$

$$\frac{dC_B}{dt} = k_1C_A - k_2C_B \tag{10}$$

$$\frac{dC_C}{dt} = k_3C_A + k_2C_B \tag{11}$$

where k_1 , k_2 , and k_3 are the reaction rate constants of conversions of A to B, B to C, and A to C, t is the reaction time, while C_A , C_B , and C_C are the concentration of A–C, respectively, based on the measurement of residual organic carbon.

The solution of these differential equations is represented by Equations (12)–(14):

$$C_A = C_{A0} \cdot e^{-(k_1+k_3) \cdot t} \tag{12}$$

$$C_B = \left(\frac{k_1}{k_1 - k_2 + k_3} \right) \cdot C_{A0} \cdot \left[e^{-k_2 \cdot t} - e^{-(k_1+k_3) \cdot t} \right] \tag{13}$$

$$C_C = C_{A0} \cdot \left[\varphi \cdot \left(e^{-(k_1+k_3) \cdot t} - 1 \right) - \left(\frac{k_1}{k_1 - k_2 + k_3} \right) \cdot \left(e^{-k_2 \cdot t} - 1 \right) \right] \tag{14}$$

where C_{A0} is the initial TOC-based concentration of A, while φ is defined in Equation (15):

$$\varphi = \frac{k_1k_2 - k_1k_3 + k_2k_3 - k_3^2}{k_1^2 - k_1k_2 + 2k_1k_3 - k_2k_3 + k_3^2} \tag{15}$$

At the start ($t = 0$), all the organic carbon present in the liquid phase (TOC_0) comes from p-cresol only, as shown in Equation (16):

$$TOC_0 = C_{A0} \tag{16}$$

At any other instant ($t > 0$), all the organic carbon present in the organic phase (TOC) is given by the sum of concentrations of residual (not yet oxidized) p-cresol plus non-

refractory intermediates resulting from its oxidation (A), which are still susceptible to oxidation, and all organic refractories difficult to mineralize and mainly consisting of simple acidic compounds (formic and acetic acid) [47] (B) (Equation (17)):

$$TOC_{(t)} = C_A + C_B \quad (17)$$

By substituting Equations (12), (13) and (16) into Equation (17), we obtain:

$$\frac{TOC_{(t)}}{TOC_0} = \left(\frac{k_1}{k_1 - k_2 + k_3} \right) \cdot e^{-k_2 \cdot t} - \left(\frac{k_2 - k_3}{k_1 - k_2 + k_3} \right) \cdot e^{-(k_1 + k_3) \cdot t} \quad (18)$$

An optimization process was applied to the experimental data in order to obtain the values of k_1 , k_2 , and k_3 from this equation.

Finally, the activation energy (E_a) was estimated using the Arrhenius equation (Equation (19)) relating the kinetic rate constant (k) of any chemical reaction (in gas or in liquid phase) to the absolute reaction temperature (T):

$$k = k_0 e^{-\frac{E_a}{R} \left(\frac{1}{T} - \frac{1}{T_0} \right)} \quad (19)$$

where k_0 is the reaction rate constant at a reference temperature T_0 and R is the constant of ideal gas.

3. Results

3.1. Optimization of Kinetic Variables

p-Cresol degradation in liquid phase was performed using hydrogen peroxide as an oxidant agent at different temperatures and dissolved oxygen levels varying the air flowrate according to the 2^3 -full factorial design described in the Section 2.

Figures 2 and 3 illustrate the time evolution of p-cresol and TOC conversions, respectively, under the investigated experimental conditions. The results obtained at different temperatures ($60 \leq T \leq 80$ °C) for a reaction time of up to 180 min show the great influence of this independent variable on both responses, with the highest conversions of p-cresol (76%) and TOC (27%) being achieved at the highest temperature (80 °C) using R of 75% and F of $150 \text{ m}^3/\text{h}$, respectively. To better elucidate the influence of R and F, a statistical analysis of the results from this experimental design was performed using the Statistic 8.0 software, by comparing the combined effects of these variables.

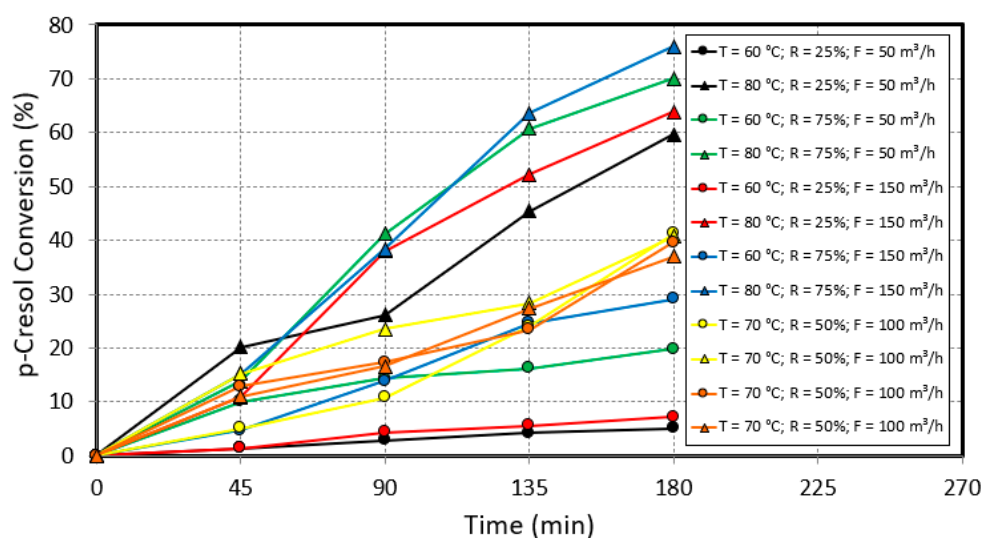


Figure 2. Time evolution of p-cresol conversion during oxidation runs carried out according to the 2^3 -full factorial design outlined in Table 1. T = temperature; R = stoichiometric ratio p-cresol/hydrogen peroxide; F = air flowrate.

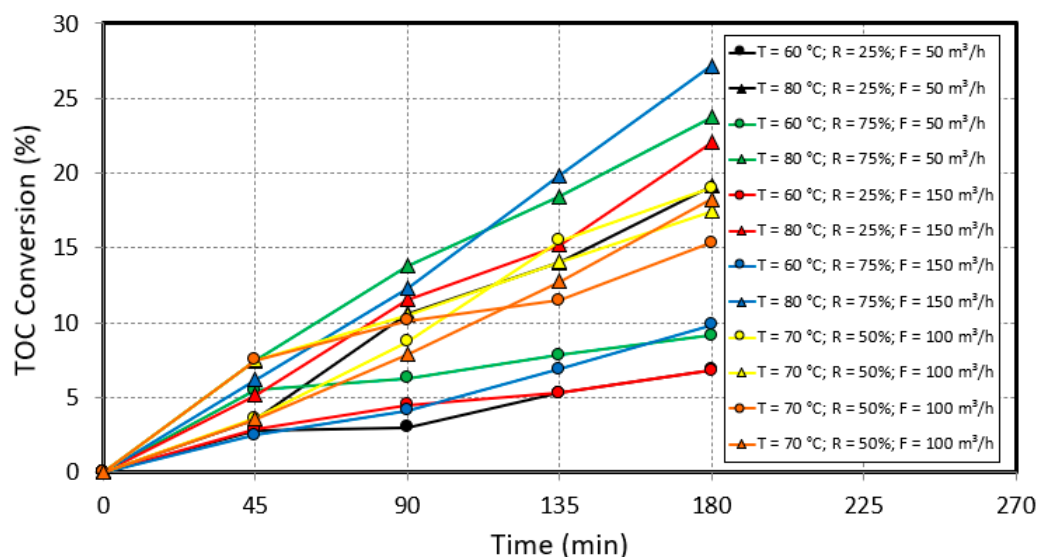


Figure 3. Time evolution of TOC during oxidation runs carried out according to the 2³-full factorial design outlined in Table 1. T = temperature; R = stoichiometric ratio p-cresol/hydrogen peroxide; F = air flowrate.

For this purpose, the Pareto charts of Figure 4A,B illustrate the dependence of the p-cresol and TOC conversions, respectively, on the selected process variables, in a 95% confidence interval. In particular, it can be seen that all three independent variables exerted statistically significant influences on p-cresol conversion, whereas only T and R did so on TOC conversion. On the other hand, second and third order interactions between variables did not statistically significantly influence both responses.

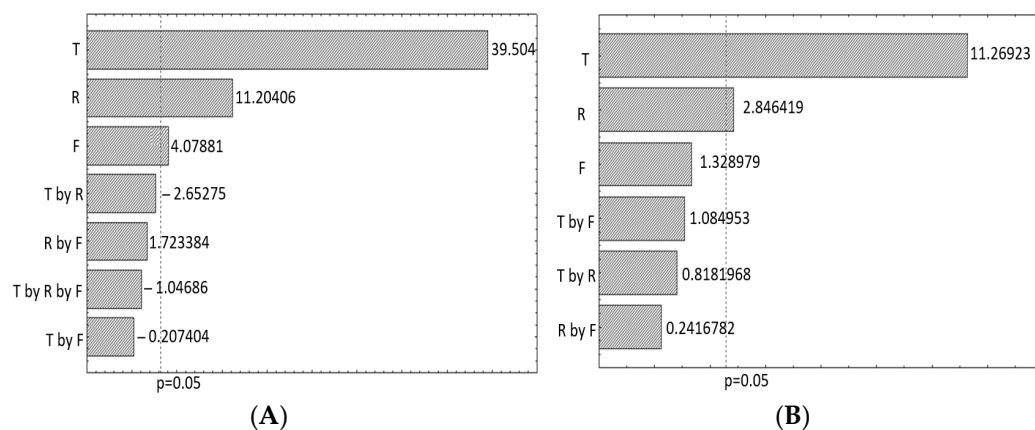


Figure 4. Pareto charts of linear and combined effects of independent variables, namely (1) temperature (T), (2) molar stoichiometric ratio of p-cresol/hydrogen peroxide (R), and (3) air flowrate (F) on: (A) p-cresol conversion; (B) TOC conversion. Runs were carried out for a reaction time of 180 min according to the 2³-full factorial design outlined in Table 1.

T was confirmed to be the most impacting parameter on p-cresol oxidation, followed by R, then by F (Figure 4A). Since the lack of adjustment to the linear model was not significant in the investigated ranges, such a response variable perfectly fitted the linear model, indicating that it would still be possible to improve the reaction yield, since the maximum inflection point has not yet been reached. As for the TOC conversion, lack of adjustment to the linear model was not significant, but it exhibited lack of adjustment to the quadratic one, which suggested that the selected conditions were far from the optimal ones and that it would be necessary to approach the optimum point with the lowest number

of additional experiments as possible. One method that allows the achievement of this goal is the Maximum Ascending Gradient Method (MAGM). Therefore, it was necessary to plan additional experiments that would run perpendicularly to the linear level curves. For this purpose, ranges of T, R, and F from the central point were enlarged by 10 °C, 7%, and 5 F h⁻¹ compared to the 2³-full factorial design, respectively. Although the influence of F on TOC conversion was not statistically significant, it was on p-cresol degradation; therefore, this factor was maintained in subsequent statistical analysis.

Table 5 shows the matrix of the adopted MAGM design as well as the results of both response variables under these conditions. From the third run onwards, the increase in temperature from 70 to 90 °C allowed a significant increase in p-cresol and TOC conversion, but the rate of water evaporation in the organic solution increased too. Therefore, to minimize water evaporation in the process, it was decided not to raise it above 90 °C, considering acceptable a water evaporation rate of up to 11% under these operating conditions.

Table 5. Conditions and results of runs carried out according to the MAGM design.

Run	Increment	T (°C)	R (%)	F (L h ⁻¹)	p-Cresol Conversion(%)	TOC Conversion(%)
1	Cx _i	70	50	100	39.65	17.48
2	Cx _i + Δx _i	80	57	105	80.58	30.80
3	Cx _i + 2Δx _i	90	64	110	99.92	52.10
4	Cx _i + 3Δx _i	90	71	115	100.00	60.86
5	Cx _i + 4Δx _i	90	78	120	100.00	64.27
6	Cx _i + 5Δx _i	90	85	125	99.80	57.15
7	Cx _i + 6Δx _i	90	92	130	99.62	53.88
8	Cx _i + 7Δx _i	90	100	135	99.17	50.15

T = temperature; R = molar stoichiometric ratio of p-cresol/hydrogen peroxide; F = air flowrate. Cx_i = central point of the coded variable x_i.

The results of Table 5 and Figure 5 show that p-cresol conversion reached very high levels in runs 3 to 8. As the difference among p-cresol conversions in these runs was very small, it was considered that optimization of p-cresol oxidation was already achieved under the reaction conditions of run 3 (T = 90 °C, R = 64%, and F = 110 L h⁻¹).

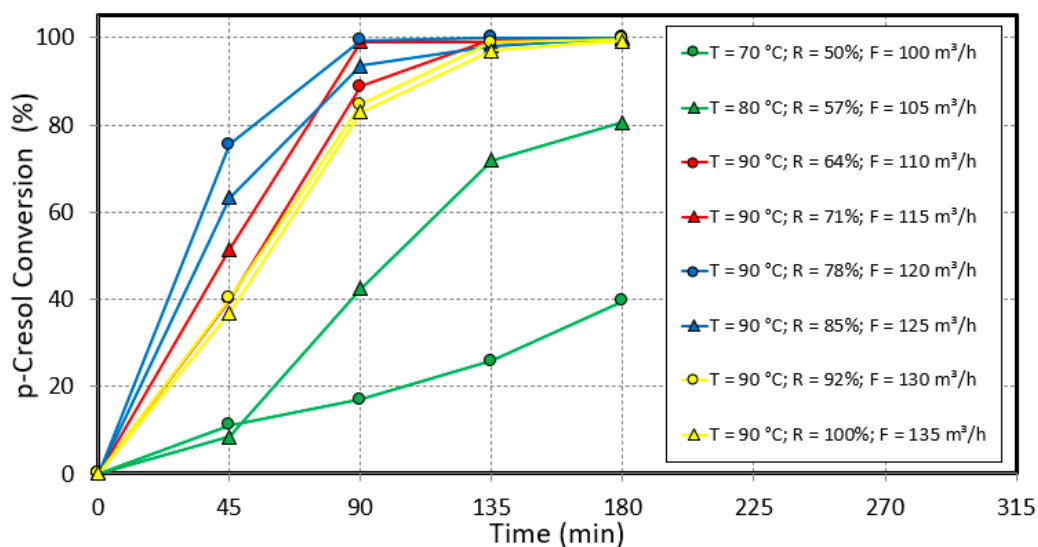


Figure 5. Time evolution of p-cresol conversion during oxidation runs carried out according to the MAGM design outlined in Table 2. T = temperature; R = stoichiometric ratio p-cresol/hydrogen peroxide; F = air flowrate.

On the other hand, the maximum TOC conversion (approximately 64%) was reached in run 5 (Table 5 and Figure 6). Comparing these results with those obtained with the 2^3 -full factorial design, maximum conversions of p-cresol and TOC increased from 76 to 100% and from 27 to 64%, respectively, which reveals the excellent ability of the MAGM to optimize process conditions.

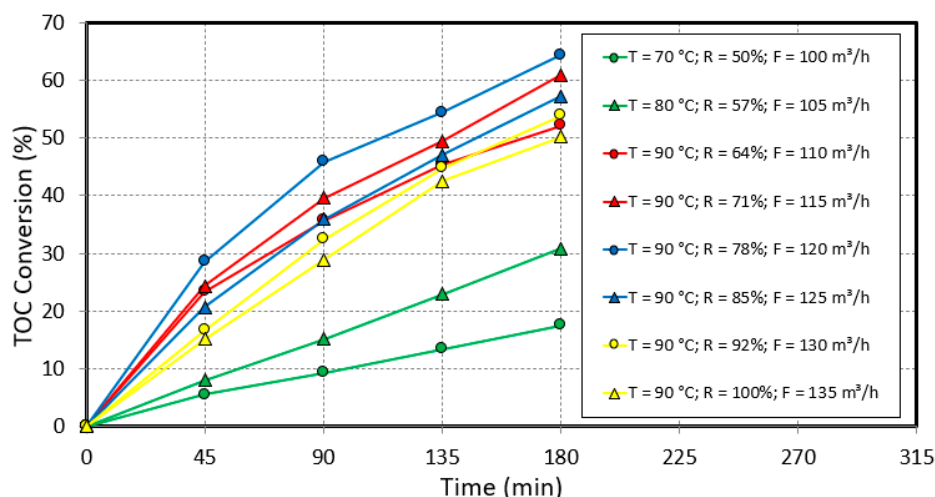


Figure 6. Time evolution of TOC during oxidation runs carried out according to the MAGM design outlined in Table 2. T = temperature; R = stoichiometric ratio p-cresol/hydrogen peroxide; F = air flowrate.

Nonetheless, exact optimization of this response was not yet achieved and should have been expected close to the reaction conditions of run 5 of the MAGM design ($T = 90\text{ }^{\circ}\text{C}$, $R = 78\%$ and $F = 120\text{ L h}^{-1}$). Based on these results, four additional runs were performed according to a 2^2 -factorial design (Table 3) under conditions around those of the above run 5 while maintaining the same conditions for the four repetitions at the central point.

According to the Pareto chart of linear and combined effects of R and F on TOC conversion (Figure 7), only the effect of the former independent variable was statistically significant. Since the lack of fit to the linear model was significant, the quadratic model was able to fit the experimental data, which means that the inflection point of the curve (optimal conversion point) should have been around the center point. Therefore, a Rotational Central Composite Design (RCCD) was additionally adopted (Table 4), in which the axial points determined with the Statistic 8.0 software were added, together with an additional central point run, to the runs of the 2^2 -factorial design (Table 3).

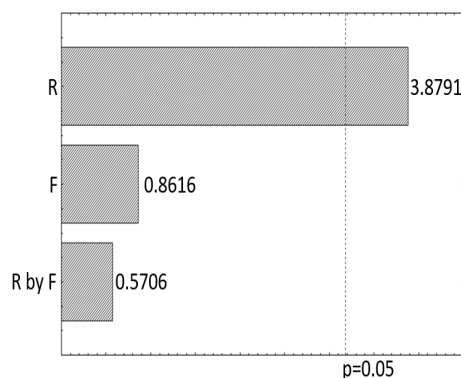


Figure 7. Pareto chart of linear and combined effects of independent variables, namely (1) molar stoichiometric ratio of p-cresol/hydrogen peroxide (R), and (2) air flowrate (F) on TOC conversion. Runs were carried out for a reaction time of 180 min according to the 2^2 -factorial design outlined in Table 3.

The contour plot (Figure 8A), level curves (Figure 8B), and prediction profiles (Figure 8C) of TOC conversion as a function of the significant variables (R and F) revealed for this response a maximum value of approximately 64% when using R of 78% and F of 120 L h⁻¹. On the other hand, the Pareto chart constructed from the RCCD (Figure 9A) shows that TOC conversion was statistically significantly influenced by the linear term of R (positively) and by the quadratic terms of R and F (both negatively). Therefore, it was possible to find an empirical model capable of representing TOC conversion (X_{TOC}) as a function of both R (64% ≤ R ≤ 100%) and F (110 L h⁻¹ ≤ F ≤ 135 L h⁻¹) (Equation (20)):

$$X_{TOC} = -3.98 \times 10^2 + 2.75 R - 2.13 \times 10^{-2} R^2 + 5.76 F - 2.61 \times 10^{-2} F^2 + 6.43 \times 10^{-3} R \times F \quad (20)$$

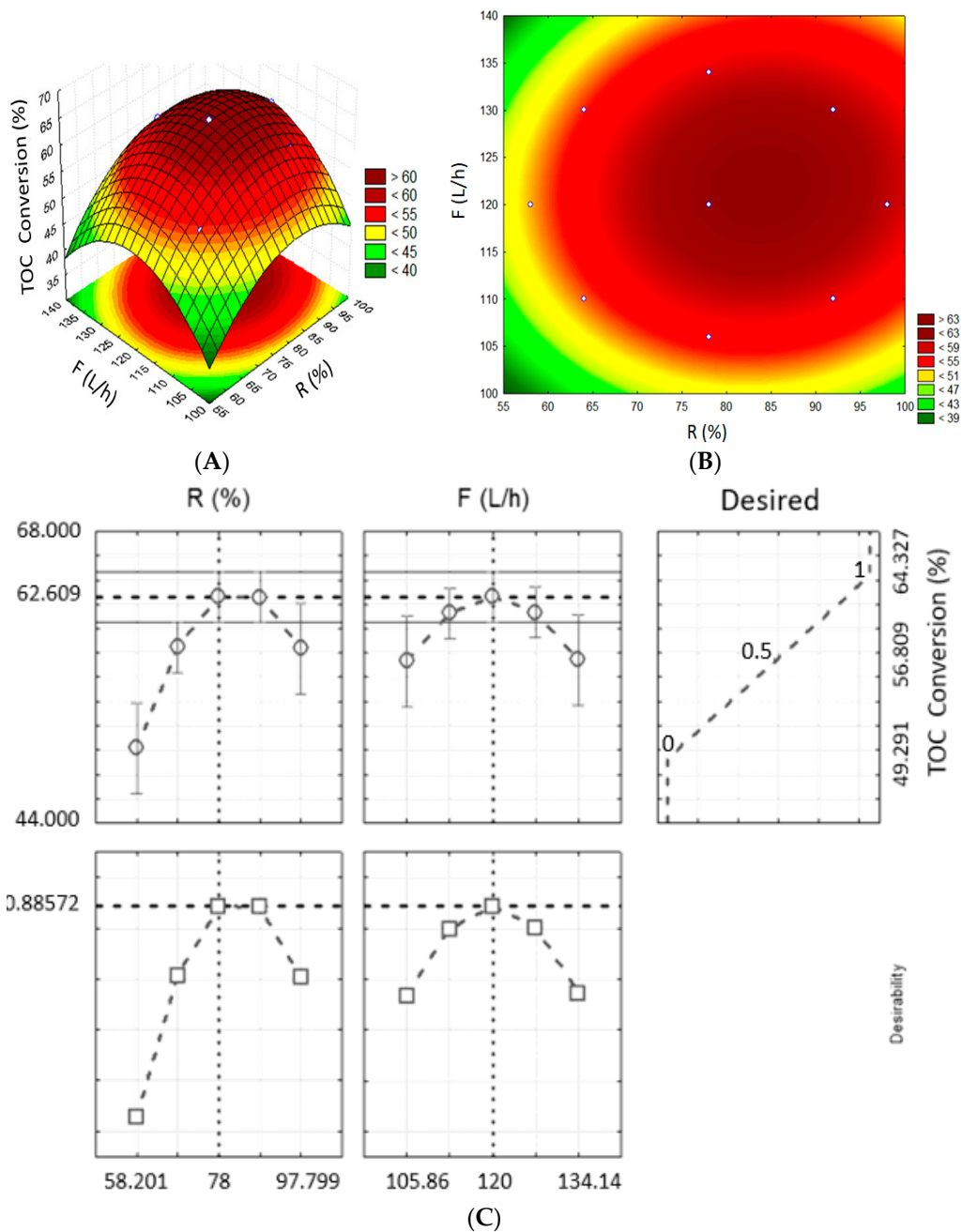


Figure 8. TOC conversion as function of molar stoichiometric ratio of p-cresol/hydrogen peroxide (R) and air flowrate (F): (A) Response surface showing the contour plot; (B) level curves; (C) prediction profiles.

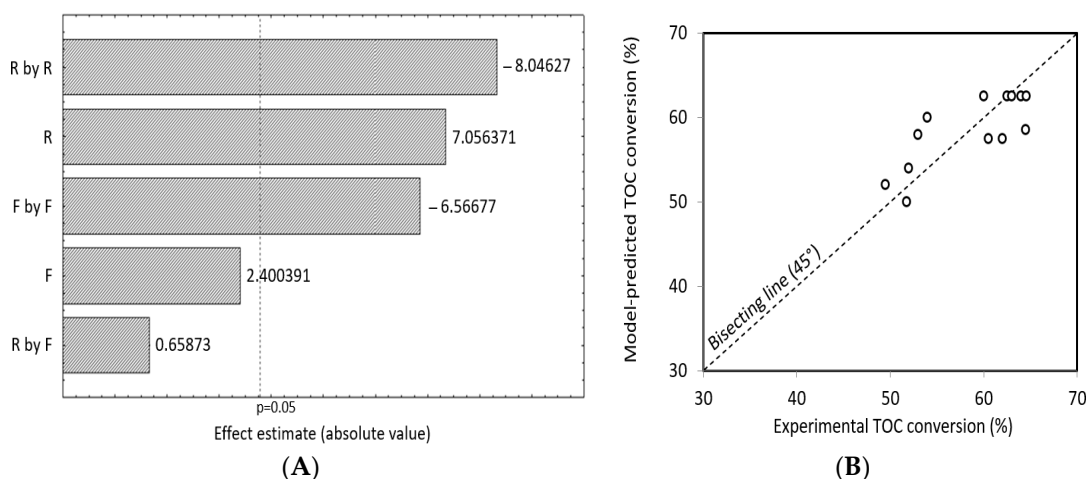


Figure 9. (A) Pareto chart of linear and combined effects of independent variables, namely molar stoichiometric ratio of p-cresol/hydrogen peroxide (R), and air flowrate (F) on TOC conversion. (B) TOC conversion values predicted by the model (Equation (19)) versus those experimentally determined. Runs were carried out for a reaction time of 180 min according to the Rotational Central Composite Design outlined in Table 4.

Figure 9B shows TOC conversion values predicted by the model through this equation versus those experimentally determined.

The application of the desirability function to the experimental data pointed to the following conditions as the optimal ones for TOC conversion: $T = 90\text{ }^{\circ}\text{C}$, $R = 78\%$, and $F = 120\text{ L h}^{-1}$. Figure 8C shows a critical point prediction for TOC conversion (X_{TOC}) from R and F. The upper curves (on the left and middle) show the predicted conversion (vertical scale) as a function of R and F (horizontal scales). The lower curves (on the left and middle) show the result of the Desirability function (vertical scale) as a function of the input variables R and F (horizontal scales). The curves correlated to the stoichiometric ratio p-cresol/peroxide (upper and lower left) show inflection within a range of values ($78 < R < 88\%$), indicating increased TOC conversion in this range. However, the Desirability function achieved the highest value ($d = 0.88572$) for $R = 78\%$, suggesting that this value of R optimizes TOC conversion ($X_{\text{TOC}} = 62.6\%$). The curves correlated to air flow (upper and lower center) suggest maximum points ($d = 0.88572$, $X_{\text{TOC}} = 62.6\%$) for $F = 120\text{ L/h}$. The upper curve (on the right) suggests that the maximum value for TOC conversion of approximately 64% ($d = 1$) can be achieved for optimized values of R and F.

3.2. Kinetics of p-Cresol Oxidation

At this stage, due to the characteristics of AOP, the mechanisms of chemical reactions become quite complex, since a large number of intermediate chemical species are formed. Some species are also oxidized in the process, generating new compounds, while others (refractory or not) are greatly resistant to the process, and many of them are very difficult to detect and quantify.

The objective of this phase of the study was to find the kinetic parameters of these chemical reactions when conducted in an industrial-scale reactor in order to elucidate the involved phenomena. Due to the above drawbacks, a lumped kinetic approach was preferred, specifically the Lumped Kinetic Model (LKM) proposed by Li et al. [46].

For this purpose, Table 6 gathers the results of TOC conversion versus time collected either at the optimum conditions for the oxidation reaction ($T = 90\text{ }^{\circ}\text{C}$, $R = 78\%$, $F = 120\text{ L h}^{-1}$) or at lower temperature ($80\text{ }^{\circ}\text{C}$), while Table 7 lists the values of the kinetic rate constants of the hypothesized reactions (Equations (7) and (8)) estimated by Equation (18) using these experimental data. Since a raise in temperature increases TOC conversion and ensures greater precision in TOC measurement, the temperature of $90\text{ }^{\circ}\text{C}$ was selected as the op-

timal one for the process, while 80 °C was selected to have a second temperature value necessary for activation energy estimation.

Table 6. Results of TOC conversion experiments along a reaction time of up to 240 min. Experimental conditions: R = 78% and F = 120 L h⁻¹.

Time (min)	T = 80 °C			T = 90 °C		
	TOC (mg L ⁻¹)	TOC/TOC ₀	TOC Conversion (%)	TOC (mg L ⁻¹)	TOC/TOC ₀	TOC Conversion (%)
0	387.20	1.00	0.00	382.93	1.00	0.00
10	376.53	0.97	2.75	369.33	0.96	3.55
20	370.75	0.96	4.25	352.80	0.92	7.87
30	354.59	0.92	8.42	337.33	0.88	11.91
40	344.08	0.89	11.14	320.53	0.84	16.30
50	331.20	0.86	14.46	290.67	0.76	24.09
60	326.61	0.84	15.65	274.93	0.72	28.20
80	304.99	0.79	21.23	237.87	0.62	37.88
100	292.48	0.76	24.46	204.80	0.53	46.52
120	273.07	0.71	29.48	185.25	0.48	51.62
140	251.81	0.65	34.97	165.68	0.43	56.73
180	220.16	0.57	43.14	148.93	0.39	61.11
240	212.05	0.55	45.23	124.34	0.32	67.53

T = Temperature.

Table 7. Values of the kinetic rate constants of overall p-cresol oxidation according to the scheme of Equations (7) and (8). Experimental conditions: R = 78% and F = 120 L h⁻¹. Estimation was done using the experimental data listed in Table 6 using Equation (18).

Kinetic Constant	T = 80 °C	T = 90 °C
k_1 (min ⁻¹)	3.19×10^{-1}	4.73×10^{-1}
k_2 (min ⁻¹)	2.99×10^{-3}	5.52×10^{-3}
k_3 (min ⁻¹)	0.00	0.00

k_1 = kinetic constant of p-cresol plus non-refractory intermediates transformation to refractory organic intermediate compounds; k_2 = kinetic constant of mineralization of refractory organic intermediate compounds to CO₂ and water; k_3 = kinetic constant of direct mineralization of p-cresol plus non-refractory intermediates to CO₂ and water.

k_3 was zero at both temperatures (Table 7), which means that, according to the scheme of Equations (7) and (8), a direct mineralization of p-cresol plus non-refractory intermediates (A) did not occur under the tested conditions, but they were rather transformed into other organic refractory compounds (B), and part of these additionally converted into CO₂ (C) and water.

It was then possible to estimate, through Equation (19), the activation energies of the reactions involved according to the proposed kinetic model (Equations (7) and (8)). The activation energy of the transformation of p-cresol plus non-refractory intermediates (A) to refractory compounds (B), (E_{a1}) was 42.02 kJ mol⁻¹, while that of direct mineralization of refractory compounds (B) to CO₂ (C) and H₂O (E_{a2}) was 65.48 kJ mol⁻¹.

Since the values of k_1 were about two orders of magnitude higher than those of k_2 at both temperatures and $k_3 = 0$ (Table 7), Equation (18) simplified to:

$$\frac{TOC(t)}{TOC_0} = e^{-k_2 \cdot t} \quad (21)$$

Table 8 shows the values of k_2 resulting from a new optimization done using the same experimental data but Equation (21) instead of Equation (18), as well as that of the activation energy of refractory compounds mineralization estimated again using Equation (19).

Table 8. Values of the kinetic rate constant of mineralization of refractory compounds to CO₂ (k_2) according to the scheme of Equations (7) and (8). Experimental conditions: R = 78% and F = 120 L h⁻¹. Estimation was done using the experimental data listed in Table 6 using Equation (21).

Reaction Temperature (°C)	k_2 (min ⁻¹)	E_{a2} (kJ mol ⁻¹)
80	2.82×10^{-3}	62.94
90	5.09×10^{-3}	

The TOC conversion (X_{TOC}) function is given by Equation (22):

$$X_{TOC} = 1 - e^{-k_2 \cdot t} \quad (22)$$

Figures 10–12 show that the experimental results were satisfactorily fitted by the model described by Equation (22), with coefficients of determination of 0.973 and 0.981 at a temperature of 80 and 90 °C, respectively.

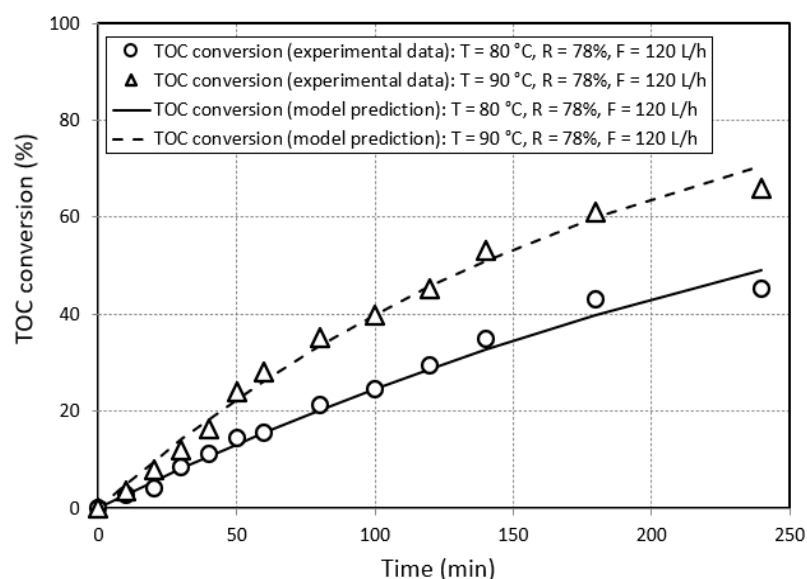


Figure 10. Adjustment of the experimental data to the kinetic model (Equation (22)). T = temperature, R = stoichiometric ratio p-cresol/hydrogen peroxide, F = air flowrate.

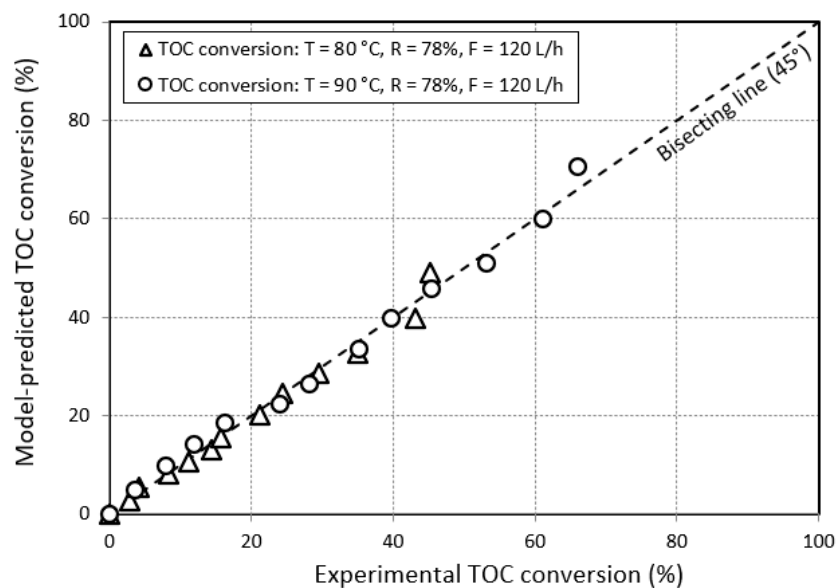


Figure 11. TOC conversion values predicted by the model (Equation (22)) versus those experimentally determined. T = temperature, R = stoichiometric ratio p-cresol/hydrogen peroxide, F = air flowrate.

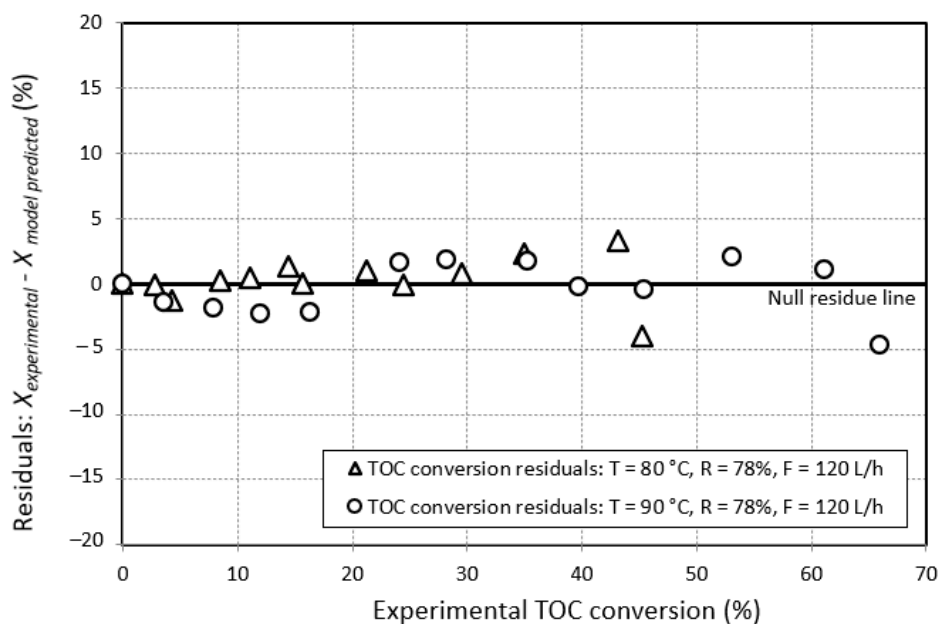


Figure 12. Residuals for the TOC conversion according to Equation (22). T = temperature, R = stoichiometric ratio p-cresol/hydrogen peroxide, F = air flowrate.

4. Discussion

Several technologies that are already commercialized are reported in the literature for the treatment of contaminated organic and refractory effluents [48]. The processes developed for the treatment of liquid waste can be divided into three types: biological, physical, and chemical, often in combination with each other. AOPs have stood out as a new alternative in the treatment of phenolic compounds, with p-cresol being one of the most common contaminants of the phenolic class.

Tian et al. [49] studied persulfate-based AOP for organic wastewater treatment. The in situ generation of highly active sulfate radical ($\bullet\text{SO}_4^-$) by activation of persulfate through conventional and emerging methods allowed to mineralize organic contaminants into carbon dioxide, water, and simple inorganic chemicals.

Ji et al. [50] reviewed perovskite oxides as heterogeneous catalysts using AOP to decompose refractory pollutants. These catalysts proved to be able to activate oxidants and produce reactive oxygen species with great redox potential and degrade pollutants in water. However, the use of perovskite-based AOPs has some limitations, such as leaching of metal ions, small surface area, low number of active sites, etc.

To treat wastewater, Iliuta and Iliuta [14] studied the biodegradation of phenol and phenol/p-cresol using a gas-liquid packed-bed column bioreactor containing *Pseudomonas putida* cells located on a packaging surface using microparticles. The results showed that the proposed intensified process was very effective, allowing high conversions of both contaminants.

Shim et al. [23] investigated the removal of p-cresol and tylosin in wastewater using novel composite alginate beads made up of alginate, activated carbon, and MnO_2 from the recycling of lithium-ion batteries. In 10 h experiments, the composite proved to be highly efficient (99%) in the removal of these emerging contaminants, whose adsorption was successfully described by the Langmuir isotherm model and pseudo second-order kinetic model.

Tessmer et al. [51] successfully treated p-cresol-containing phenolic compounds by oxidative coupling reactions and adsorption onto activated carbon in the presence of dissolved oxygen. This study showed that, due to acidic functional groups on activated carbon surface, the adsorption of phenolic organic compounds is limited, thus reducing the efficiency of the AOP/adsorption coupled process.

Alvarez et al. [52] described the use of a Granular Activated Carbon (GAC) composite to immobilize anthraquinone-2-sulfonate, subsequent removal of Congo red by incubation in a batch reactor, and degradation of *p*-cresol in a Upflow Anaerobic Sludge Blanket (UASB) reactor. In the batch reactor, approximately 2.64 times more decolorization was obtained than using GAC combined with quinone (anthraquinone-2-sulfonate)-containing substances, while the UASB reactor ensured decolorization efficiencies ranging from 79.9 to 83.9%.

Brandão et al. [20] recently reported an unconventional AOP, called Direct Contact Thermal Treatment (DiCTT), which, using the combustion of natural gas and excess air, acts as a thermochemical process capable of ensuring complete degradation of phenol and very high TOC conversions. Three variables were analyzed, namely initial phenol concentration (500, 1000, and 1500 mg L⁻¹), molar stoichiometric ratio of phenol/hydrogen peroxide (25, 50, and 75%), and reaction time (30, 90, and 150 min), while the liquid phase flowrate, burner power dissipation, air excess, and recycle rate of gaseous thermal wastes were set at 170 L h⁻¹, 38.6 kW, 10%, and 100%, respectively. The DiCTT proved to be very efficient with a phenol degradation as high as 99% and a TOC conversion > 40%.

The same DiCTT gave similar results (maximum phenol degradation of 100% and TOC conversion > 30%) in the treatment of the same contaminants under different operating conditions, namely natural gas flow rate of 2–4 m³ h⁻¹, air excess of 10–50%, and recycling rate of the combustion gases of 0–100% [35].

Teodosio et al. [29] investigated the same AOP used in this study at an initial hydroquinone concentration of 500 mg L⁻¹ using a batch reactor. Optimization and kinetic modeling were carried out to identify the conditions ensuring the highest hydroquinone degradation and TOC conversion. The kinetic model used to describe the profile of the TOC conversion was the LKM. Thus, the values of the speed constants for hydroquinone reaction were k_1 (0.076 min⁻¹), k_2 (0.012 min⁻¹), and k_3 (0 min⁻¹). Using a reaction time of 180 min, the following parameters were varied to optimize the process: initial pH, T, F, and R. After the application of the MAGM, hydroquinone degradation and TOC conversion under optimized conditions (pH = 9.3, T = 90 °C, R = 110%, and F = 50 L h⁻¹) were approximately 100 and 84%, respectively, showing the exceptional efficiency of the process.

At pressure between 5 and 200 atm and temperature between 127 and 300 °C oxidation of organic compounds occurs using oxygen without catalyst. Zimpro, Wetox, Vertech, and Kenox processes are based on this procedure, named Wet Air Oxidation (WAO). On the other hand, the oxidizing agent used in this study was hydrogen peroxide (H₂O₂), which decomposes into hydroxyl radical when submitted to heating in the reaction medium [53].

Napoleão [54] studied the emerging contaminants using AOP with ultraviolet and hydrogen peroxide (UV/H₂O₂) and obtained the highest TOC conversion (practically 100%) under its optimum operating conditions (H₂O₂ volume = 4 µL; pH = 6–7; T = 30 °C; pressure = 1 atm). The LKM kinetic model was also applied to describe the profile of the total residual concentration in terms of carbon contained in the liquid phase. The values obtained showed in the LKM the kinetic constants for the mineralization of the drugs plus the non-refractory intermediates ($k_3 = 0.0402$ min⁻¹), the degradation of the drugs plus the non-refractory intermediates to refractory intermediates ($k_1 = 0.0546$ min⁻¹), and the mineralization of the refractory intermediates ($k_2 = 0.0023$ min⁻¹). Although there is a large temperature difference compared with our non-photo-reactional tests, the values of k_1 and k_2 are of the same order of magnitude.

Britto and Rangel [55] studied the kinetics and oxidation mechanism of phenol and substituted phenols using oxygen as an oxidizing agent. Using temperatures in the range of 25 to 80 °C, these authors estimated activation energies for the oxidation reactions in the range between 5.44 and 54.01 kJ mol⁻¹.

Kavitha and Palanivelu [56], who used the conventional Fenton process to degrade the three isomeric forms of cresol, estimated global activation energies in the range between 12.90 and 16.25 kJ mol⁻¹.

Finally, Kshirsagar et al. [57], who studied the kinetics of p-cresol oxidation in liquid phase for the production of p-hydroxybenzaldehyde using cobalt oxide (Co_3O_4) as a catalyst, estimated an activation energy for this catalytic reaction of 39.6 kJ mol^{-1} .

The results of the present study pointed out again the importance of the treatment of aqueous streams containing toxic organic and refractory substances, being an efficient decontamination process. This process has as its main attraction the demonstrated ability to oxidize phenolic compounds, especially p-cresol, at low temperatures and atmospheric pressure in a vertical reactor in a compact configuration that can be installed on offshore oil platforms where physical space is limited. Many of the organic compounds treatments used in cited works have limitations regarding the selectivity in the treatment of liquid effluents. Certain factors, such as the concentration of organic matter and temperature may adversely affect the efficiency of such processes. Some effluents require storage and disposal of the removed contaminants. The results obtained in this work showed greater degradation of p-cresol (almost 100%) and TOC conversion (almost 64%) compared for example with that of Teodosio et al. [29], who used the same reactor to treat hydroquinone. Comparison can also be made with the research of Brandão et al. [35], who applied an unconventional advanced oxidation process (AOP), called Direct Contact Thermal Treatment (DiCTT), able to oxidize phenolic compounds using natural gas as an energy source. Almost complete phenol degradation (>99%) and TOC conversion (>30%) for a given evaporation rate to the liquid phase (<11%) and effluent temperature (70–78 °C) were obtained under optimal conditions. Thus, this research proves once again the effectiveness of this process under optimal operating conditions in degrading p-cresol (100%) and convert TOC (64%), promising to be able to achieve even better performance in future works.

5. Conclusions

In the present work, the use of a batch reactor to perform in situ p-cresol oxidation was proposed, which allowed almost complete degradation and 63% TOC conversion within 180 min under optimal conditions, i.e., a reaction temperature (T) of 90 °C, a stoichiometric ratio of p-cresol/hydrogen peroxide (R) of 78%, and an air flowrate (F) of 120 L h^{-1} . T was shown to be the most impacting parameter on the TOC conversion, followed by R, while F had some influence only in combination with R. The so-called Lumped Kinetic Model (LKM) was used to model the kinetics of p-cresol oxidation hypothesizing a complex reaction scheme including (i) conversion of p-cresol to refractory organic compounds, (ii) mineralization of refractory compounds to CO_2 , and (iii) direct mineralization of p-cresol to CO_2 . Initially, a nonlinear regression using the overall model applied to the results obtained at $T = 80 \text{ °C}$, $R = 78\%$, and $F = 120 \text{ L h}^{-1}$ allowed calculating kinetic rate constants for the transformation of p-cresol to refractory compounds (k_1) and refractory compounds to CO_2 (k_2) of $3.19 \times 10^{-1} \text{ min}^{-1}$ and $2.99 \times 10^{-3} \text{ min}^{-1}$, respectively, while that of direct mineralization of p-cresol to carbon dioxide and water (k_3) was insignificant. Increasing the temperature to 90 °C, while maintaining R and F at the same levels, k_1 and k_2 were $4.73 \times 10^{-1} \text{ min}^{-1}$ and $5.52 \times 10^{-3} \text{ min}^{-1}$, respectively. The Arrhenius law was used to estimate the activation energies (E_a) of both reactions (i) and (ii), which were $42.02 \text{ kJ mol}^{-1}$ and $65.48 \text{ kJ mol}^{-1}$, respectively. These results demonstrate that, within the operating conditions tested in this work, direct p-cresol mineralization practically did not occur, and that this pollutant was converted into other organic substances, which were then partially mineralized. A final attempt was then made omitting k_3 in the overall kinetic equation, which allowed calculating the k_2 of 2.82×10^{-3} and 5.09×10^{-3} at 80 and 90 °C, respectively, and $E_a = 62.94 \text{ kJ mol}^{-1}$.

The elaboration of advanced kinetics for organic pollutants oxidation, followed by quantification of kinetic rate constants of reactions and activation energies, is of great importance to develop in situ processes on offshore platforms to treat contaminants, in particular, those polluting seawater, before being discharged into the oceans. These treatments would in fact allow not only a significant reduction of environmental pollution, but also important energy savings for the oil and natural gas sector.

Author Contributions: Conceptualization, Y.B.B. and M.B.; methodology, J.G.C.O. and J.R.T.; software, D.C.O. and J.G.C.O.; validation, C.M.M., Y.B.B. and L.A.S.; formal analysis, M.B. and D.C.O.; investigation, C.M.M. and L.A.S.; resources, Y.B.B.; data curation, A.A.C. and A.C.; writing—original draft preparation, J.G.C.O. and Y.B.B.; writing—review and editing, J.R.T., A.A.C., A.C., L.A.S. and C.M.M.; visualization, D.C.O., A.A.C. and A.C.; supervision, J.R.T. and M.B.; project administration, Y.B.B., M.B. and L.A.S.; funding acquisition, Y.B.B., M.B., L.A.S. and A.A.C. All authors have read and agreed to the published version of the manuscript.

Funding: The study was conducted with financial support for the research project from the Coordenação de Aperfeiçoamento de Pessoal de Nível Superior (CAPES (Coordination for Advancement of Higher Education Personnel—Finance code 001)), Universidade Federal de Pernambuco and Instituto Avançado de Tecnologia e Inovação (IATI (Advanced Institute of Technology and Innovation)). The authors are also grateful to Conselho Nacional de Desenvolvimento Científico e Tecnológico (CNPq (National Council of Scientific and Technological Development)).

Acknowledgments: This work was developed as part of a thesis to be presented to the Programa de Pós-Graduação em Engenharia Química (PPGEQ (Postgraduate Program in Chemical Engineering)) of Universidade Federal de Pernambuco (UFPE).

Conflicts of Interest: The authors declare no conflict of interest.

References

1. Sheng, J.; Voldsund, M.; Ertesvåg, I.S. Advanced exergy analysis of the oil and gas processing plant on an offshore platform: A thermodynamic cycle approach. *Energy Rep.* **2023**, *9*, 820–832. [CrossRef]
2. De Oliveira, S., Jr.; Van Hombeeck, M. Exergy analysis of petroleum separation processes in offshore platforms. *Energy Convers. Manag.* **1997**, *38*, 1577–1584. [CrossRef]
3. Kayadelen, H.K. Effect of natural gas components on its flame temperature, equilibrium combustion products and thermodynamic properties. *J. Nat. Gas Sci. Eng.* **2017**, *45*, 456–473. [CrossRef]
4. Neff, J.; Lee, K.; DeBlois, E.M. Produced water: Overview of composition, fates, and effects. In *Produced Water: Environmental Risks and Advances in Mitigation Technologies*, 1st ed.; Lee, K., Neff, J., Eds.; Springer: New York, NY, USA, 2011; Volume 18, pp. 4–5.
5. Al-Kaabi, M.A.; Zouari, N.; Da'Na, D.A.; Al-Ghouti, M.A. Adsorptive batch and biological treatments of produced water: Recent progresses, challenges, and potentials. *J. Environ. Manag.* **2021**, *290*, 112527. [CrossRef] [PubMed]
6. Faksness, L.-G.; Grini, P.G.; Daling, P.S. Partitioning of semi-soluble organic compounds between the water phase and oil droplets in produced water. *Mar. Pollut. Bull.* **2004**, *48*, 731–742. [CrossRef] [PubMed]
7. Chittick, E.A.; Srebotnjak, T. An analysis of chemicals and other constituents found in produced water from hydraulically fractured wells in California and the challenges for wastewater management. *J. Environ. Manag.* **2017**, *204*, 502–509. [CrossRef]
8. Neto, S.L.d.C.; Viviani, J.C.T.; Weschenfelder, S.E.; Cunha, M.d.F.R.d.; Junior, A.E.O.; Costa, B.R.D.S.; Mazur, L.P.; Marinho, B.A.; da Silva, A.; de Souza, A.A.U.; et al. Evaluation of petroleum as extractor fluid in liquid-liquid extraction to reduce the oil and grease content of oilfield produced water. *Process. Saf. Environ. Prot.* **2022**, *161*, 263–272. [CrossRef]
9. Brandão, Y.; Teodosio, J.; Benachour, M.; Oliveira, J.; Marinho, I.; Figueirêdo, F.; Anselmo-Filho, P. Estudo do efeito do excesso de ar e da potência dissipada do queimador sobre as capacidades do processo DiCTT no tratamento de efluentes líquidos fenólicos. *Rev. Ibero-Am. Sist. Cibernética E Inf.* **2010**, *7*, 1–9.
10. Fedorov, K.; Plata-Gryl, M.; Khan, J.A.; Boczkaj, G. Ultrasound-assisted heterogeneous activation of persulfate and peroxymonosulfate by asphaltenes for the degradation of BTEX in water. *J. Hazard. Mater.* **2020**, *397*, 122804. [CrossRef]
11. Saikia, S.; Gogoi, R.D.; Yadav, M.; Yadav, H.S. Isolation, purification and characterization of peroxidase from *Raphanus sativus* and its applications in biotransformation of cresols. *Biocatal. Agric. Biotechnol.* **2022**, *46*, 102540. [CrossRef]
12. Jun, L.Y.; Yon, L.S.; Mubarak, N.; Bing, C.H.; Pan, S.; Danquah, M.K.; Abdullah, E.; Khalid, M. An overview of immobilized enzyme technologies for dye and phenolic removal from wastewater. *J. Environ. Chem. Eng.* **2019**, *7*, 102961. [CrossRef]
13. Benali, M.; Guy, C. Thermochemical oxidation of phenolic-laden liquid effluent models. *J. Environ. Eng. Sci.* **2007**, *6*, 543–552. [CrossRef]
14. Iliuta, I.; Iliuta, M.C. Intensified phenol and p-cresol biodegradation for wastewater treatment in countercurrent packed-bed column bioreactors. *Chemosphere* **2021**, *286*, 131716. [CrossRef] [PubMed]
15. Singh, R.K.; Kumar, S.; Kumar, S.; Kumar, A. Biodegradation kinetic studies for the removal of p-cresol from wastewater using *Gliomastix indicus* MTCC 3869. *Biochem. Eng. J.* **2008**, *40*, 293–303. [CrossRef]
16. Duan, W.; Meng, F.; Cui, H.; Lin, Y.; Wang, G.; Wu, J. Ecotoxicity of phenol and cresols to aquatic organisms: A review. *Ecotoxicol. Environ. Saf.* **2018**, *157*, 441–456. [CrossRef]
17. China Chemical Safety Association. Available online: <https://www.aiche.org/content-source/china-chemical-safety-association> (accessed on 15 May 2023).
18. Helcom. *Response to Accidents at Sea Involving Spills of Hazardous Substances and Loss of Packaged Dangerous Goods*; Baltic Marine Environment Protection Commission: Helsinki, Finland, 2002; pp. 64–87.

19. Wei, X.; Gilevska, T.; Wetzig, F.; Dorer, C.; Richnow, H.-H.; Vogt, C. Characterization of phenol and cresol biodegradation by compound-specific stable isotope analysis. *Environ. Pollut.* **2016**, *210*, 166–173. [CrossRef]
20. Brandão, Y.B.; Oliveira, D.C.; Dias, F.F.S.; Teodosio, J.R.; Oliveira, J.G.C.; Oliveira, C.G.C.; Moraes, C.M.; Araújo, L.A.; Benachour, M. Thermochemical advanced oxidation process by DiCTT for the degradation/mineralization of effluents phenolics with optimization using response surface methodology and artificial neural networks modelling. *PPEJ* **2023**, *7*, 000329. [CrossRef]
21. Liu, Z.; Xu, J.; Liu, M.; Yin, Z.; Liu, X.; Yin, L.; Zheng, W. Remote sensing and geostatistics in urban water-resource monitoring: A review. *Mar. Freshw. Res.* **2023**, *74*, 22167. [CrossRef]
22. Tian, Y.; Yang, Z.; Yu, X.; Jia, Z.; Rosso, M.; Dedman, S.; Zhu, J.; Xia, Y.; Zhang, G.; Yang, J.; et al. Can we quantify the aquatic environmental plastic load from aquaculture? *Water Res.* **2022**, *219*, 118551. [CrossRef]
23. Shim, J.; Kumar, M.; Goswami, R.; Mazumder, P.; Oh, B.-T.; Shea, P.J. Removal of p-cresol and tylosin from water using a novel composite of alginate, recycled MnO₂ and activated carbon. *J. Hazard. Mater.* **2019**, *364*, 419–428. [CrossRef]
24. Xiao, M.; Qi, Y.; Feng, Q.; Li, K.; Fan, K.; Huang, T.; Qu, P.; Gai, H.; Song, H. P-cresol degradation through Fe(III)-EDDS/H₂O₂ Fenton-like reaction enhanced by manganese ion: Effect of pH and reaction mechanism. *Chemosphere* **2021**, *269*, 129436. [CrossRef]
25. Aziz, F.; Jalil, A.; Hassan, N.; Fauzi, A.; Khusnun, N.; Ali, M.; Bahari, M.; Nabgan, W. CuO improved energy band of AgO/fibrous SiO₂-ZrO₂ for optimized simultaneous photocatalytic redox of chromium (VI) and p-cresol using response surface methodology. *Environ. Res.* **2023**, *220*, 115151. [CrossRef] [PubMed]
26. Somu, P.; Narayanasamy, S.; Gomez, L.A.; Rajendran, S.; Lee, Y.R.; Balakrishnan, D. Immobilization of enzymes for bioremediation: A future remedial and mitigating strategy. *Environ. Res.* **2022**, *212*, 113411. [CrossRef] [PubMed]
27. Razzaghi, M.; Karimi, A.; Ansari, Z.; Aghdasinia, H. Phenol removal by HRP/GOx/ZSM-5 from aqueous solution: Artificial neural network simulation and genetic algorithms optimization. *J. Taiwan Inst. Chem. Eng.* **2018**, *89*, 1–14. [CrossRef]
28. Brandão, Y.B.; Oliveira, J.G.C.; Benachour, M. Phenolic waste waters: Definition, sources and treatment processes. In *Phenolic Compounds: Natural Sources, Importance and Applications*; Soto-Hernandez, M., Tenango, M.P., García-Mateos, M.d.R., Eds.; IntechOpen: Rijeka, Croatia, 2017; Volume 1, pp. 154–196.
29. Teodosio, J.R.; Brandão, Y.B.; Oliveira, D.C.; Dias, F.F.S.; Moraes, C.M.; Araújo, L.A.; Oliveira Júnior, D.C.; Oliveira, J.G.C.; Benachour, M. Treatment of effluents containing hydroquinone in a batch reactor: Optimization technique via RSM, MAGM and kinetic modelling. *PPEJ* **2023**, *7*, 000341. [CrossRef]
30. Yang, L.; Jiao, Y.; Xu, X.; Pan, Y.; Su, C.; Duan, X.; Sun, H.; Liu, S.; Wang, S.; Shao, Z. Superstructures with atomic-level arranged perovskite and oxide layers for advanced oxidation with an enhanced non-free radical pathway. *ACS Sustain. Chem. Eng.* **2022**, *10*, 1899–1909. [CrossRef]
31. Wang, Y.; Sun, T.; Tong, L.; Gao, Y.; Zhang, H.; Zhang, Y.; Wang, Z.; Zhu, S. Non-free Fe dominated PMS activation for enhancing electro-Fenton efficiency in neutral wastewater. *J. Electroanal. Chem.* **2023**, *928*, 117062. [CrossRef]
32. Bilińska, L.; Gmurek, M.; Ledakowicz, S. Textile wastewater treatment by AOPs for brine reuse. *Process. Saf. Environ. Prot.* **2017**, *109*, 420–428. [CrossRef]
33. Renuka, M.K.; Gayathri, V. UV/solar light induced photocatalytic degradation of phenols and dyes by Fe(PS-BBP)Cl₃. *J. Photochem. Photobiol. A Chem.* **2018**, *353*, 477–487. [CrossRef]
34. Berenguer, C.F.; Brandão, Y.B.; Benachour, M. Estudo de tratamento de água em efluentes refratários por processo Fenton para degradação e mineralização desses compostos em reator de escala laboratorial modelo PARR. In *Ciência e Engenharia de Materiais*; Abdala, R.W.S., Ed.; Atena: Ponta Grossa, PR, Brazil, 2018; Volume 3, pp. 139–155.
35. Brandão, Y.B.; Dias, F.F.; Oliveira, D.C.; Zaidan, L.E.; Teodosio, J.R.; Oliveira, J.G.; Benachour, M. Unconventional advanced oxidation technique: Evaporation liquid rate and phenolic compounds degradation evaluation and modelling/optimization process with CFD, RSM and ANNs. *Fuel* **2021**, *300*, 120967. [CrossRef]
36. Li, X.; Zhou, M.; Pan, Y.; Xu, L.; Tang, Z. Highly efficient advanced oxidation processes (AOPs) based on pre-magnetization Fe 0 for wastewater treatment. *Sep. Purif. Technol.* **2017**, *178*, 49–55. [CrossRef]
37. Resolução CONAMA N0 430 de 13/05/2011. Available online: <https://www.legisweb.com.br/legislacao/?id=114770> (accessed on 15 May 2023).
38. Myers, R.H.; Montgomery, D.C.; Anderson-Cook, C.M. *Response Surface Methodology: Product and Process Op-timization Using Designed Experiments*, 2nd ed.; John Wiley and Sons: New York, NY, USA, 2002; pp. 856–863.
39. Barros Neto, B.; Scarminio, I.S.; Bruns, R.E. *Como Fazer Experimentos*, 4th ed.; Bookman: Porto Alegre, RS, Brazil, 2010; pp. 413–419.
40. Harrington, E.C., Jr. The desirability function. *Ind. Qual. Control.* **1965**, *21*, 494–498. [CrossRef]
41. Derringer, G.; Suich, R. Simultaneous optimization of several response variables. *J. Qual. Technol.* **1980**, *12*, 214–219. [CrossRef]
42. Surajit, P.; Susanta, K.G. A desirability functions-based approach for simultaneous optimization of quantitative and ordinal response variables in industrial processes. *Int. J. Eng. Sci. Technol.* **2018**, *10*, 76–87. [CrossRef]
43. Amdoun, R.; Khelifi, L.; Khelifi-Slaoui, M.; Amroune, S.; Asch, M.; Assaf-ducrocq, C.; Gontier, E. The desirability optimization methodology; a tool to predict two antagonist responses in biotechnological systems: Case of biomass growth and hyoscyamine content in elicited *Datura stramonium* hairy roots. *Iran. J. Biotechnol.* **2018**, *16*, e1339. [CrossRef]
44. Siebert, A.P.F.; Silva, A.C.B.; Moraes, C.M.; Bezerra, R.S.; Silva, L.C.M.; Oliveira, D.C.; Benachour, M.; Brandão, Y.B. Utilização da Moringa oleifera Lam e da radiação solar no tratamento de água para consumo humano. *Braz. J. Dev.* **2020**, *6*, 86102–86129. [CrossRef]

45. Brandão, Y.; Teodosio, J.; Dias, F.; Eustáquio, W.; Benachour, M. Treatment of phenolic effluents by a thermochemical oxidation process (DiCTT) and modelling by artificial neural networks. *Fuel* **2013**, *110*, 185–195. [[CrossRef](#)]
46. Li, L.; Chen, P.; Gloyna, E.F. Generalised kinetic model for wet oxidation of organic compounds. *AIChE J.* **1991**, *37*, 1687–1697. [[CrossRef](#)]
47. Devlin, H.R.; Harris, I.J. Mechanism of the oxidation of aqueous phenol with dissolved oxygen. *Ind. Eng. Chem. Res.* **1984**, *23*, 387–392. [[CrossRef](#)]
48. Saygılı, H.; Güzel, F.; Önal, Y. Conversion of grape industrial processing waste to activated carbon sorbent and its performance in cationic and anionic dyes adsorption. *J. Clean. Prod.* **2015**, *93*, 84–93. [[CrossRef](#)]
49. Tian, K.; Hu, L.; Li, L.; Zheng, Q.; Xin, Y.; Zhang, G. Recent advances in persulfate-based advanced oxidation processes for organic wastewater treatment. *Chin. Chem. Lett.* **2022**, *33*, 4461–4477. [[CrossRef](#)]
50. Ji, R.; Chen, J.; Liu, T.; Zhou, X.; Zhang, Y. Critical review of perovskites-based advanced oxidation processes for wastewater treatment: Operational parameters, reaction mechanisms, and prospects. *Chin. Chem. Lett.* **2021**, *33*, 643–652. [[CrossRef](#)]
51. Tessmer, C.H.; Vidic, R.D.; Uranowski, L.J. Impact of oxygen-containing surface functional groups on activated carbon adsorption of phenols. *Environ. Sci. Technol.* **1997**, *31*, 1872–1878. [[CrossRef](#)]
52. Alvarez, L.H.; Arvizu, I.C.; García-Reyes, R.B.; Martínez, C.M.; Olivo-Alanis, D.; Del Angel, Y.A. Quinone-functionalized activated carbon improves the reduction of congo red coupled to the removal of p-cresol in a UASB reactor. *J. Hazard. Mater.* **2017**, *338*, 233–240. [[CrossRef](#)] [[PubMed](#)]
53. Luna, A.J.; Rojas, L.O.A.; Melo, D.M.A.; Benachour, M.; de Sousa, J.F. Total catalytic wet oxidation of phenol and its chlorinated derivatives with MnO₂/CeO₂ catalyst in a slurry reactor. *Braz. J. Chem. Eng.* **2009**, *26*, 493–502. [[CrossRef](#)]
54. Napoleão, D.C. Avaliação e Tratamento dos Contaminantes Emergentes (Ácido Acetilsalicílico, Diclofenaco e Paracetamol) utilizando Processos Oxidativos Avançados. Master's Thesis, Universidade Federal de Pernambuco, Recife, Brasil, 2011.
55. Britto, J.M.; Rangel, M.D.C. Processos avançados de oxidação de compostos fenólicos em efluentes industriais. *Química Nova* **2008**, *31*, 114–122. [[CrossRef](#)]
56. Kavitha, V.; Palanivelu, K. Destruction of cresols by Fenton oxidation process. *Water Res.* **2005**, *39*, 3062–3072. [[CrossRef](#)]
57. Kshirsagar, V.; Nadgeri, J.; Tayade, P.; Rode, C. Reaction kinetics of liquid phase air oxidation of p-cresol to p-hydroxybenzaldehyde. *Appl. Catal. A Gen.* **2008**, *339*, 28–35. [[CrossRef](#)]

Disclaimer/Publisher's Note: The statements, opinions and data contained in all publications are solely those of the individual author(s) and contributor(s) and not of MDPI and/or the editor(s). MDPI and/or the editor(s) disclaim responsibility for any injury to people or property resulting from any ideas, methods, instructions or products referred to in the content.